Unique precursors for the mesenchymal cells involved in injury response and fibrosis

Janice L. Walker[a], Ni Zhai[a], Liping Zhang[a], Brigid M. Bleaken[a], Iris Wolff[a], Jacquelyn Gerhart[b], Mindy George-Weinstein[b], and A. Sue Menko[a,1]

[a]Department of Pathology, Anatomy and Cell Biology, Thomas Jefferson University, Philadelphia, PA 19107; and [b]Lankenau Institute for Medical Research, Wynnewood, PA 19096

Edited by Tadatsugu Taniguchi, University of Tokyo, Tokyo, Japan, and approved June 22, 2010 (received for review September 11, 2009)

We investigated an alternative pathway for emergence of the mesenchymal cells involved in epithelial sheet wound healing and a source of myofibroblasts that cause fibrosis. Using a mock cataract surgery model, we discovered a unique subpopulation of polyploid mesenchymal progenitors nestled in small niches among lens epithelial cells that expressed the surface antigen G8 and mRNA for the myogenic transcription factor MyoD. These cells rapidly responded to wounding of the lens epithelium with population expansion, acquisition of a mesenchymal phenotype, and migration to the wound edges where they regulate the wound response of the epithelium. These mesenchymal cells also were a principal source of myofibroblasts that emerged following lens injury and were responsible for fibrotic disease of the lens that occurs following cataract surgery. These studies provide insight into the mechanisms of wound-healing and fibrosis.

lens | myofibroblast | wound healing | migration | posterior capsule opacification

Mesenchymal cells play a central role in epithelial wound healing, fibrosis, and cancer (1–3). The emergence of cells with a mesenchymal phenotype within an epithelial sheet has been attributed to a transformation of the endogenous epithelial cells, commonly referred to as an epithelial to mesenchymal transition (EMT) (4, 5), or to cells sourced outside the epithelial tissue such as fibroblasts (6, 7), pericytes (8), and bone marrow-derived cells (9, 10). In this study, we investigate the alternate possibility that epithelia contain a subpopulation of mesenchymal precursor cells that function in epithelial wound healing and that can be signaled to differentiate into myofibroblasts. Our model for these studies is an ex vivo culture system originally developed to study the lens fibrotic disease known as posterior capsule opacification (PCO) (11). With this culture model, it is possible to follow the response of an intact epithelium to a clinically relevant wounding within a native microenvironment. Wounding of the epithelium is the result of mock cataract surgery. This microsurgical procedure involves removal of the lens fiber cell mass from within the lens capsule, a thick basement membrane that surrounds the entire lens, which leaves the posterior aspects of the lens capsule denuded of cells (diagrammed in Fig. S1). The lens epithelium remains intact and attached to the capsule with its principal wound edge bordering the area where the fiber cells had been attached (leading edge, Fig. S1). By making a few cuts in its anterior regions, creating additional wound edges (cut edge, Fig. S1), the tissue is flattened, pinned to the culture dish cell-side-up, and cultured as an ex vivo explant. This approach makes it possible to follow the response of the wounded epithelium to injury using the high resolution of confocal microscopy. The epithelial cells in this wound model quickly begin a collective migration across the denuded basement membrane capsule into the wounded area, and the wound is filled with epithelial cells within a few days in culture (11). Expression of molecular markers associated with the emergence of myofibroblasts is detected biochemically only after the wound-healing process is completed (11), demonstrating that in this ex vivo model, the development of fibrotic disease is principally a postmigratory and postwound closure event.

The hypotheses we examined in this study were: (*i*) a subpopulation of mesenchymal precursors was present among the epithelial cells of the mature lens, (*ii*) these cells could be activated upon injury to modulate the wound-healing process, and (*iii*) the progeny of these cells have the potential to become myofibroblasts, a phenotype associated with the development of fibrotic disease. The cell type we investigated as a candidate for the mesenchymal precursor cell in our lens injury model is identified by its expression of the cell-surface antigen G8 and messenger RNA (mRNA) for the skeletal muscle-specific transcription factor MyoD, but not MyoD protein. Cells with these properties were originally identified as a subpopulation of the epiblast (12–14), a tissue that gives rise to all three germ layers of the embryo (15). G8 and MyoD mRNA expressing epiblast cells are capable of undergoing myogenesis when removed from the embryo and placed in culture (12–14). In vivo, these cells are incorporated into somites where they function instead as cell-signaling centers that promote the myogenic differentiation of surrounding skeletal muscle progenitor cells through their release of Noggin, a bone morphogenetic protein inhibitor (16). $G8^{pos}$/$MyoD^{pos}$ cells also are incorporated into tissues that lack skeletal muscle (12, 17–19), including the embryonic lens (20), where our studies now suggest they play a principal role in wound repair and are a source of disease-causing myofibroblasts.

Results

We identified that $G8^{pos}$ cells were an innate subpopulation of cells of the mature lens and determined their localization, in situ, focusing on their association with the lens epithelium. To preserve the position of $G8^{pos}$ cells as exists in vivo, lenses were fixed before the preparation of lens epithelial explants. $G8^{pos}$ cells within the explants were localized by immunostaining with mAb to the G8 antigen and the cytoarchitecture of the host epithelium revealed by colabeling the explants with fluorescent-conjugated phalloidin. The labeled explants were examined by confocal microscopy (Fig. 1). $G8^{pos}$ cells were discovered localized in niches, nestled among the lens epithelial cells (Fig. 1*A*). A typical niche of $G8^{pos}$ cells (shown at higher magnification in Fig. 1*B Lower*) contained, on average, 8 cells [8 ± 1 (mean ± SEM)]. Up to 14 such niches were detected in a single epithelial explant. The positioning of the $G8^{pos}$ cell niches within the lens epithelium corresponded to the equatorial region of the intact lens. Because $G8^{pos}$ cells in other tissues typically coexpress mRNA for the myogenic transcription

Author contributions: J.L.W., M.G.-W., and A.S.M. designed research; J.L.W., N.Z., L.Z., B.M.B., I.W., and J.G. performed research; M.G.-W. contributed new reagents/analytic tools; J.L.W., M.G.-W., and A.S.M. analyzed data; and J.L.W. and A.S.M. wrote the paper.

The authors declare no conflict of interest.

This article is a PNAS Direct Submission.

[1]To whom correspondence should be addressed. E-mail: sue.menko@jefferson.edu.

This article contains supporting information online at www.pnas.org/lookup/suppl/doi:10.1073/pnas.0910382107/-/DCSupplemental.

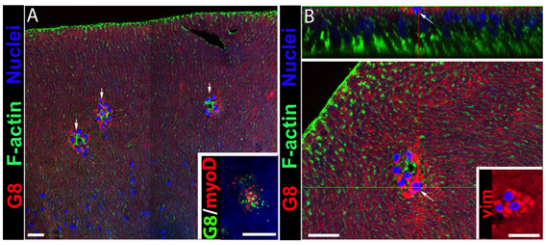

Fig. 1. G8^{pos} cell subpopulation resides in niches within the lens epithelium. Lenses were fixed at E15 before preparation of epithelial explants, preserving the in situ localization G8^{pos} cells. Explants were labeled with a mAb to the G8 antigen tagged with rhodamine-conjugated secondary antibody (red) and costained for F-actin (Alexa Fluor 488 phalloidin, green) and nuclei (TO-PRO-3, blue). Confocal imaging in a single optical plane digitally acquired as an *x–y* tile (A) showed G8^{pos} cells localized to niches (arrows) nestled among the lens epithelial cells, at higher magnification in *B*. (Scale bars: 20 μm.) (*A Inset*) Lens epithelium-associated G8^{pos} cells (green) also expressed MyoD mRNA (red), detected with DNA dendrimers conjugated to a MyoD antisense oligonucleotide sequence tagged with Cy3, in explants fixed at T0 in culture; nuclei were counterstained with Hoechst dye. To further position the G8^{pos} cell niches, an orthogonal cut (*B Upper*) was created from a *Z*-stack of consecutive 1-μm optical sections acquired apically to basally by scanning confocal imaging. The orthogonal cut was made along the green line in the representative optical section (*B Lower*). The G8^{pos} niches were associated with the apical surfaces of lens epithelial cells (arrow, *B*). (*B Inset*) Niche cells also expressed the mesenchymal marker vimentin (vim, red).

factor MyoD (12, 17–19), a property that gives cells myogenic potential (21, 22), we double-labeled epithelial explants with fluorescein-tagged G8 mAb and DNA dendrimers conjugated with both an antisense oligonucleotide sequence for MyoD mRNA and the fluorochrome Cy3 (23, 24). The results showed that the G8^{pos} cells associated with the lens epithelium also expressed MyoD mRNA (Fig. 1*A Inset*). Quantification showed that all G8^{pos} cells in the explants coexpressed MyoD mRNA (177 cells in three separate explants) and only 2% (3 of 180) of the cells that labeled with MyoD lacked detectable G8 antigen. The mesenchymal potential of these G8^{pos} cells was supported further by the discovery that this subpopulation of cells expressed vimentin before injury (Fig. 1*B Inset*).

Orthogonal sections of *Z*-stacks collected by confocal microscopy were created to investigate the localization of the G8^{pos} cell niches within the lens epithelium. This analysis revealed that niches of G8^{pos} cells were localized along the apical surfaces of the lens epithelial cells (see arrow in Fig. 1*B Upper*). The unique localization of the G8^{pos} cell niches placed these mesenchymal precursors in position to function as rapid responders to injury of the host epithelium. The presence of a subpopulation of G8^{pos} cells innate to epithelia was not limited to embryonic lenses or to avian species because subpopulations of G8^{pos} cells also were present in lens epithelial explants from newborn and adult rats (Fig. S2 and Fig. S3).

A central aspect of this study was to examine the response of G8^{pos} mesenchymal precursor cells to injury. For these studies, the lens epithelium was wounded by mock cataract surgery and placed in culture as ex vivo explants (Fig. S1). The response of the G8^{pos} precursor cells at 1 h after injury of the epithelium was determined by confocal imaging of explants costained for the G8 antigen and F-actin (Fig. 2 *A–E*). Image analysis revealed that within this short time period postinjury, G8^{pos} cells had emerged from their niches (Fig. 2*A*) and migrated toward the leading edge (Fig. 2*B*). Observation of the G8^{pos} cells in orthogonal sections of collected *Z*-stacks showed that G8^{pos} cells were migrating along the apical surfaces of the lens epithelium (Fig. 2*C*). Most striking was the finding that a population of G8^{pos} cells already had reached the wound edges within 1 h after injury, a response seen at both the leading edge adjacent to where the fiber cells had been removed (Fig. 2 *C* and *D*) and the cut edge where the epithelium had been flattened (Fig. 2*E*). Similar rapid response to injury of the G8^{pos}/vimentin^{pos} mesenchymal precursor population occurred in adult rat lens epithelia (Fig. S3). The active migration of G8^{pos} cells to the wound edge was confirmed through time-lapse imaging (Movie S1 and Fig. S4). The G8^{pos} cells that had emerged from the niches continued to express the mesenchymal protein vimentin (Fig. 2 *G* and *H*), but MyoD protein still was not detected in these cells (Fig. S5 *A* and *B*). ZO-1, a protein characteristic of epithelial junctions, localized to the apical cell–cell borders of lens epithelial cells, but not to the G8^{pos} cells responding to wounding of the epithelium (Fig. S6), further evidence of the mesenchymal phenotype of these activated G8^{pos} cells. These results demonstrated that the subpopulation of G8^{pos} mesenchymal precursor cells responded rapidly to injury of the lens epithelium by emerging from their niches and migrating to the wound edges.

Another unique and unusual property of the mesenchymal progenitor population was their rapid expansion in response to

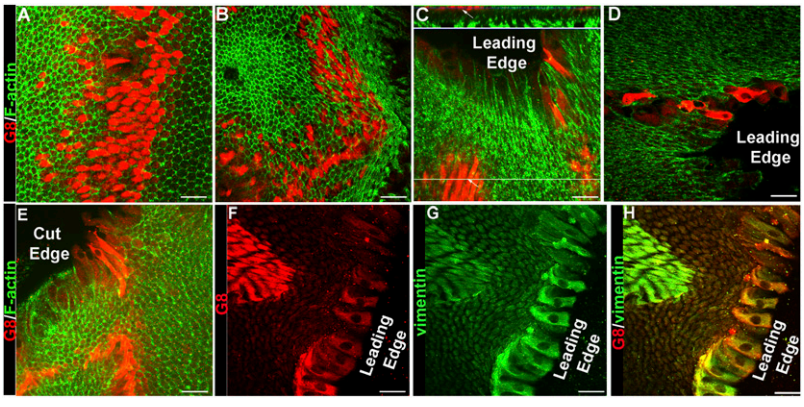

Fig. 2. G8^{pos} precursor cells emerge from niches and migrate to wound edges in response to injury of the epithelium. (*A–E*) The initial response of G8^{pos} cells to injury was determined at 1 h in culture in media containing serum by immunolabeling with G8 mAb (red). Staining of F-actin with Alexa Fluor 488-phalloidin (green) outlined lens epithelial cells. Injury inflicted by mock cataract surgery induced rapid emergence of G8^{pos} cells from their niches (*A*) and their migration toward the leading edge (*B*). Orthogonal cut (*C Upper*) through a confocal *Z*-stack at the position of the green line (*C Lower*) showed that G8^{pos} cells (arrow) migrated to the leading edge along apical surfaces of lens epithelial cells. In this short time after injury, G8^{pos} cells already had reached the wound edges, both the leading edge (*C* and *D*) and the cut edge (*E*) of the explant. (*F–H*) Mesenchymal phenotype of G8^{pos} cells responding to injury was demonstrated by double-labeling for G8 (*F*, red) and vimentin (*G*, green), overlain in *H*. (Scale bars: 20 μm.)

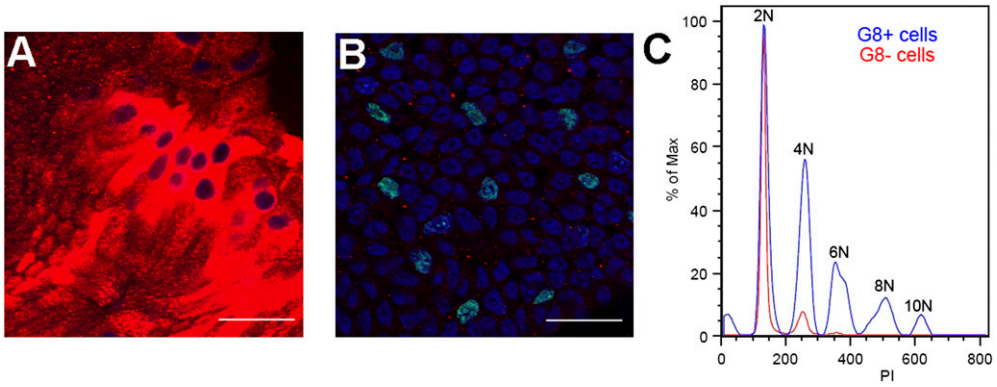

Fig. 3. Mechanism of rapid expansion of G8 cells. To determine whether expansion of the G8^{pos} cells in response to wounding involved their rapid proliferation, we performed the fluorescent EdU DNA synthesis assay (green) over the first hour after wounding. Cultures were double-labeled with antibody to G8 (red) and nuclei-stained with TO-PRO-3 (blue). No EdU-positive nuclei were detected in G8 expanded cell niches after injury (*A*); however, there was significant DNA replication in the lens epithelial cell population (*B*). (Scale bars: 20 μm.) To examine whether the G8^{pos} cells have a greater than 2N complement of DNA that would allow them to divide without DNA replication, cells were isolated from the lens, labeled with antibody to G8 and propidium iodide (PI), and analyzed by flow cytometry (*C*). The results show that a large number of G8^{pos} cells (G8+, blue) had a greater than 2N complement of DNA, with some G8^{pos} cells having as much as a 10N DNA complement. Lens cells (G8-, red) were primarily diploid with a small number of cells with a 4N DNA complement.

wounding. The average number of G8^{pos} cells per niche expands from 8 ± 1 cells before injury to 48 ± 5 G8^{pos} cells at 1 h postinjury. This expansion occurred without DNA replication, because G8^{pos} cells failed to incorporate 5-ethynyl-2′-deoxyuridine (EdU) during the first hour after wounding (Fig. 3*A*). In contrast, wounding did induce the lens epithelial cells to replicate their DNA (Fig. 3*B*), as

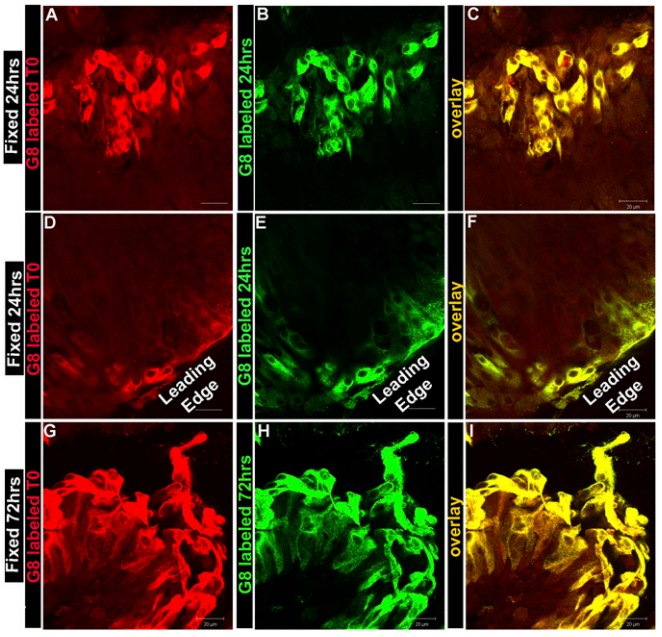

Fig. 4. Tracking studies show that G8^{pos} cells responding to injury of the lens epithelium were progeny of G8^{pos} cells present at the time of wounding. G8^{pos} cells in lens epithelial ex vivo explants were tagged at T0 with G8 mAb and a rhodamine-conjugated secondary antibody. Explants with tagged G8 cells were incubated and the G8 cells tracked for 24 h (*A–F*) or 72 h (*G–I*) after the time of injury, at which time they were fixed and labeled again with the G8 mAb, this time tagged with an Alexa Fluor 488-conjugated secondary antibody. *A–C* and *G–I* are expanded niches, and *D–F* are cells at leading edge. All cells that labeled with the Alexa Fluor 488-tagged G8 (*B*, *E*, and *H*) also were labeled with the tracked rhodamine-tagged G8 (*A*, *D*, and *G*), as seen in the overlays (*C*, *F*, and *I*). These results demonstrated that the G8^{pos} cells that participated in healing of the lens epithelium were derived from the G8^{pos} precursor cells present at the time of injury and did not include cells later recruited to the G8 lineage. (Scale bars: 20 μm.)

is needed for their repopulation of the wound area. To investigate further how the G8^{pos} progenitor population was poised to expand so rapidly in response to injury, we examined the ploidy of these cells by flow cytometry (Fig. 3*C*). Surprisingly, not only were there many G8^{pos} cells with a 4N complement of DNA, but a high number of these cells had a 6N complement, and a smaller number of G8^{pos} cells had up to at least 10N DNA complement. This unique phenotype would allow G8^{pos} cells to divide without first progressing through the S phase of the cell cycle.

Throughout the wound-healing process, which takes ~3 d, G8^{pos} cells were found clustered along the apical surfaces of the lens epithelium as well as at the wound edges. To investigate whether the G8^{pos} cells that responded to epithelial wounding were indeed progeny of the G8^{pos} cells present at time 0 (T0, immediately after microsurgery), G8^{pos} cells were tagged at T0 with G8 antibody and a rhodamine-conjugated secondary antibody and tracked during the period of wound closure. At both 24 h (Fig. 4 *A–F*) and 72 h (Fig. 4 *G–I*) in culture, the explants were fixed and the G8^{pos} cells present at these times were immunostained with the G8 mAb tagged with an Alexa Fluor 488-conjugated secondary antibody. During active wound healing (24 h), all G8^{pos}/Alexa Fluor 488-labeled cells also labeled with the G8-rhodamine tag, whether the G8^{pos} cells were located in clusters along the epithelium (Fig. 4 *A–C*) or had migrated to the leading wound edge (Fig. 4 *D–F*). Even as wound healing was completed (72 h), all G8^{pos}/Alexa Fluor 488-labeled cells were colabeled with the G8-rhodamine tag (Fig. 4 *G–I*). These results demonstrated that the G8^{pos} cells involved in the wound-healing response of the lens epithelium were derived from the population of G8^{pos} cells present at T0.

Healing of the wounded lens epithelium (wound closure) occurs before molecules associated with fibrosis, such as α-smooth muscle actin (α-SMA) and fibronectin, are detected biochemically (11). However, within days after the wound has closed, expression of both of these molecules is induced and α-SMA-positive cells with a mesenchymal morphology typical of emerging myofibroblasts appear among the lens epithelial cells (11). We now investigated whether the G8^{pos} cells that were activated in response to injury of the lens epithelium were the precursors of the myofibroblasts that appeared at later times in our ex vivo injury model. A myofibroblast is defined as a mesenchymal cell that has organized α-SMA into stress fibers (7, 25), a feature that provides these cells with the contractile function that links them to fibrotic diseases like PCO. To examine whether G8^{pos} cells were precursors of the myofibroblasts that emerge in our culture model, we performed image

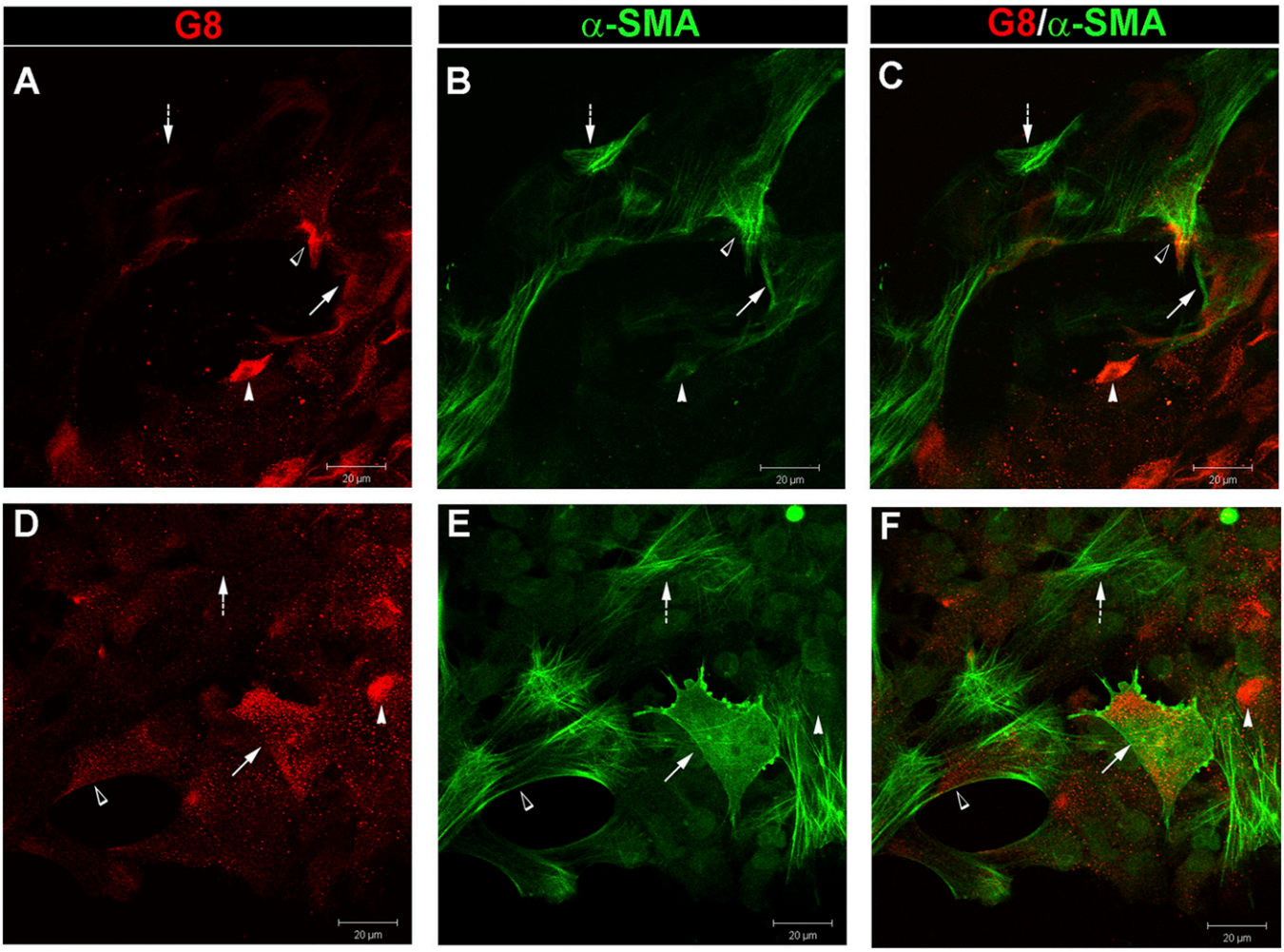

Fig. 5. G8^{pos} cells are myofibroblast precursors. Wounded lens epithelia cultured for 6 d (*A–C*) were double-labeled for G8 antigen (red, *A*) and α-SMA (green, *B*) (overlain in *C*). Within colonies of G8^{pos} cells there was a progression from G8^{pos} cells to myofibroblasts: G8^{pos} cells expressing little to no α-SMA (white arrowhead), G8^{pos} cells expressing α-SMA not yet organized into stress fibers (arrow), G8^{pos} cells with α-SMA containing stress fibers (open arrowhead), and myofibroblasts that had lost the G8 antigen (dashed arrow). Explants also were grown under conditions that permitted G8^{pos} cells to migrate onto the rigid culture dish, promoting differentiation of G8 cells to myofibroblasts within 3 d (*D–F*), in the same progression noted above. (Scale bars: 20 μm.)

analysis on ex vivo explants that were cultured under serum-free conditions, fixed on culture day 6, immunolabeled with the G8 mAb and a rhodamine-conjugated secondary antibody, and colabeled with an α-SMA antibody directly conjugated to fluorescein (Fig. 5 *A–C*). Confocal imaging revealed the presence of G8^{pos} cells that contained α-SMA-positive stress fibers, demonstrating that G8^{pos} cells were indeed a source of myofibroblasts in this wound model. Cells that had differentiated into myofibroblasts also expressed protein for MyoD (Fig. S5 *C* and *D*). We discovered that there was a progression from G8^{pos} precursor cell to myofibroblast within small clusters of G8^{pos} cells associated with the epithelium. The transitional cell types included G8^{pos} cells with little to no expression of α-SMA (white arrowhead), G8^{pos} cells that expressed α-SMA not yet organized into stress fibers (arrow), and G8^{pos} cells containing α-SMA positive stress fibers (open arrowhead), the G8-expressing myofibroblasts. This study also demonstrated that a final step in the differentiation of G8 cells to myofibroblasts was loss of the precursor cell antigen G8 (dashed arrow). The loss of a precursor cell marker upon differentiation is a feature these cells share with the differentiated progeny of many precursor cell populations (26, 27).

Next, we examined whether it was possible to push the G8^{pos} cells to differentiate into myofibroblasts. For these studies we took advantage of the fact that myofibroblast development is known to be enhanced in rigid environments (28) and grew the ex vivo cultures in serum containing media that permitted G8^{pos} cells at the cut edge to migrate from the lens capsule onto the rigid culture dish. This population of G8^{pos} cells was examined for expression of α-SMA in G8^{pos} cells at culture day 3, a time point before α-SMA-positive myofibroblasts had emerged within their native microenvironment of the lens epithelium. The transition from G8^{pos} precursor cells to α-SMA-positive myofibroblasts was promoted when the G8^{pos} cells came in contact with a rigid substrate (Fig. 5 *D–F*). The process of transition from G8^{pos} cell to myofibroblast was the same as described above for emergence of myofibroblasts on the lens capsule. These data demonstrate that G8^{pos} cells give rise to myofibroblasts.

Lastly, we examined whether α-SMA expression was suppressed in the ex vivo cultures when G8^{pos} cells were eliminated on the first day in culture by labeling them with the G8 antibody and lysing them with complement. Cell lysis in the treated cultures was confirmed by trypan blue uptake, as this dye is excluded from live cells. Trypan blue staining was detected in small colonies of cells (Fig. 6*A*, G8+C, ablation; see encircled large colony at the leading edge). The distribution of the trypan blue labeled colonies resembled that of the expanded colonies of

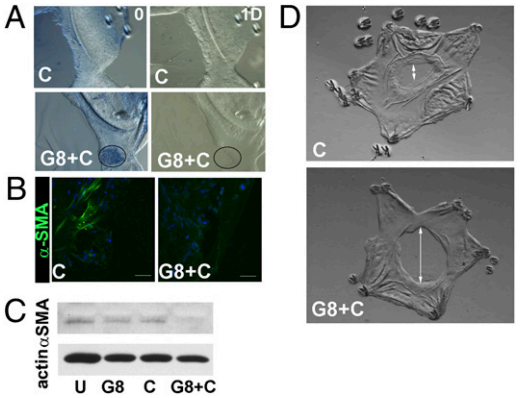

Fig. 6. Wound healing and fibrosis following ablation of G8^{pos} cells. (*A–D*) G8^{pos} cells were ablated in epithelial explants at culture day 1 by tagging them with G8 mAb (G8) and lysing them with complement (*C*). (*A*) Trypan blue uptake marks area of lysed cells (encircled area) in G8+C compared with C, confirmed by cell loss at 1 d postablation. (*B*) Epithelial explants were exposed to G8+C or C alone at culture day 1, cultured another 5 d, and immunostained for αSMA. (*C*) Explants were exposed to G8+C, C alone, G8 alone, or left untreated (U) at culture day 1, cultured another 5 d, and immunoblotted for α-SMA and β-actin. In both studies, ablation of G8 cells blocked expression of α-SMA. (*D*) Migration of the leading wound edge to fill the wounded area was followed by light microscopy for 5 d postablation. Double arrow denotes region on basement capsule remaining open. Ablation of G8^{pos} cells resulted in impaired cell migration and wound healing.

G8^{pos} cells typically present at culture day one. Twenty-four hours after ablation, lysis was confirmed by the subsequent loss of cells from regions that had stained for trypan blue (Fig. 6*A*, G8+C, 1 day postablation). Similar cell loss was not observed in control cultures incubated with complement alone (Fig. 6*A*). Immunostaining for the G8 antigen after 5 d in culture postablation demonstrated that this approach effectively removed most G8^{pos} cells (Fig. S7). At 6 d in culture, untreated control explants typically express α-SMA, as shown here by immunoblot analysis (Fig. 6*C*). In cultures in which G8^{pos} cells were ablated (G8+C), expression of α-SMA was suppressed, whereas in cultures exposed to G8 antibody (G8) or complement alone (C), there was little effect on α-SMA expression. Immunolocalization studies confirmed the loss of α-SMA-positive myofibroblasts after ablation of G8^{pos} cells (Fig. 6*B*). These results provide further evidence that G8^{pos} cells are the precursors of myofibroblasts.

The ablation studies also revealed the effect of loss of G8^{pos} cells on the wound-healing process. Removal of G8^{pos} cells after injury by ablation resulted in an aberrant wound-healing response, evidenced by slowed migration of the lens epithelium across the wound area and, therefore, the failure of the wound to close at a normal rate (Fig. 6*D*).

Discussion

In this study, we report our discovery that a distinct subpopulation of mesenchymal precursor cells were present in niches localized among the cells of the lens epithelium. This cell type rapidly responded to injury of the epithelium and had the potential to differentiate into myofibroblasts. Unique features of these cells included their polyploidy, their expression of the cell-surface antigen G8, and their expression of mRNA for MyoD, the last an indicator of their myogenic potential. After wounding of the lens epithelium, the G8^{pos} subpopulation quickly emerged from their niches, expanded in population size, exhibited a mesenchymal phenotype, and migrated to the wound edge. The presence of mesenchymal cells at the wound edge is a characteristic of many epithelial wound-healing models, but their appearance is typically attributed to an EMT or to a cell source outside of the epithelium. Our studies of the wounded lens epithelium revealed an alternate paradigm where a population of G8^{pos}/MyoD^{pos} precursor cells innate to the epithelium are the progenitors of the mesenchymal cells that responded to injury and localized to the wound edge. This same precursor population can differentiate into myofibroblasts, whose appearance after wounding is associated with the development of fibrotic disease. This finding was of particular importance to the development of the lens fibrotic disease PCO, a consequence of wounding of the lens epithelium during cataract surgery. The presence of small subpopulations of cells that express the G8 antigen and/or MyoD in other tissues prone to fibrosis such as the lung, liver, and kidney (12, 29) suggests that the ability of activated G8^{pos}/MyoD^{pos} cells to differentiate into myofibroblasts contributes to the development of fibrosis in many tissues.

Materials and Methods

Ex Vivo Epithelial Explant Preparation. To prepare ex vivo epithelial explants, lenses were removed from embryonic day (E)15 chicken embryo (Truslow Farms and B&E Eggs) eyes by dissection (11). Then, an incision was made in the anterior lens capsule, the thick basement membrane that surrounds the lens, from which the lens fiber cell mass was removed by hydroelution. This process, in which the lens epithelium remains tightly adherent to the capsule, mimics cataract surgery. The principle wound edge (leading edge) of the epithelium borders the area where the fiber cells had been attached (model, Fig. S1). Cuts were made in the anterior region of this tissue, creating additional wound edges that allowed the explants to be flattened and pinned to the culture dish cell-side-up (Fig. S1). The response of the lens epithelium to wounding within their native microenvironment was followed by microscopic imaging. The ex vivo epithelial explants were cultured in Media 199 (Invitrogen) containing 1% pen-strep (Mediatech-Cellgro) and 1% L-glutamine (Mediatech-Cellgro) with or without 10% FCS (Invitrogen) as specified. A similar approach was used for preparation of rat ex vivo lens explants. In experiments designed to preserve the position of the G8^{pos} cells as they occur in vivo, lenses were fixed for 10 min in 3.7% formaldehyde before preparing the epithelial explants.

Immunofluorescence and in Situ Hybridization. Epithelial explants were immunostained as described in ref. 11. Briefly, explants were fixed in 3.7% formaldehyde in PBS and permeabilized in 0.25% Triton X-100 in PBS before immunostaining. Cells were incubated with primary antiserum followed by rhodamine (Jackson Laboratories and Millipore), fluorescein (Jackson Laboratories), or Alexa Fluor 488 (Invitrogen-Molecular Probes) conjugated secondary antibodies. The following primary antibodies were used for the immunofluorescence studies: G8 mAb (12), vimentin (mAb; Developmental Studies Hybridoma Bank), vimentin (polyclonal) antibody (a generous gift from Paul FitzGerald, University of California, Davis), MyoD (Vector Labs), ZO-1 (Invitrogen), and fluorescein (FITC)-conjugated α-SMA mAb (Sigma). Some explants were counterstained with Alexa Fluor 488-conjugated phalloidin, which binds filamentous actin, and TO-PRO 3, a nuclear stain (Invitrogen-Molecular Probes). All immunostained samples were examined with a confocal microscope (LSM 510; Zeiss) except those that were also processed for in situ hybridization. Either single images or *Z*-stacks were collected and analyzed; the data presented represent single optical planes or orthogonal sections imaged from the apical to basal direction.

For in situ hybridization studies, mRNAs for MyoD were detected with DNA dendrimers conjugated with Cy3 and the following antisense oligonucleotide sequence: chicken MyoD, 5′-TTCTCAAGAGCAAATACTCACCATTTGGTGATTC-CGTGTAGTA-3′ (Genisphere) as described in refs. 23 and 24. Explants were double-labeled for the G8 antigen, counterstained with Hoechst, and examined with an epifluorescence microscope (Eclipse E800; Nikon). Images were captured with a video camera (Evolution QE; Media Cybernetics) and Image-Pro Plus software (Phase 3 Imaging Systems).

Cell Tracking. G8 cells were labeled for tracking according to procedure described in ref. 16. Briefly, the lens ex vivo epithelial explants were incubated at T0 in Media 199 containing the G8 mAb (1:40) for 45 min at room temperature, rinsed in Media 199, and incubated in rhodamine-conjugated IgM antibody (Millipore) for 30 min at room temperature. The labeled explants were rinsed in Media 199, placed in serum-free media (SFM) (Media 199 containing 1% Pen strep and L-glutamine) and incubated at 37 °C. After 24 or 72 h in culture, the epithelial explants were fixed in 3.7% formaldehyde. To determine whether G8^{pos} cells that responded to epithelial wound

healing 24 or 72 h postinjury were indeed progeny of $G8^{pos}$ cells present at T0, the fixed explants were labeled again with the G8 mAb (1:40), this time followed by an IgM secondary antibody conjugated to Alexa Fluor 488 (Invitrogen-Molecular Probes). Previous fate mapping studies in which $G8^{pos}$ cells are tracked from the epiblast to embryonic tissues demonstrate that G8 mAb that tags $G8^{pos}$ cells in the epiblast remains associated with these cells throughout the study and does not transfer to surrounding cells (16). A similar labeling protocol was used for the time-lapse studies, and images were acquired with a Coolsnap HQ camera (Photometrics) on a Nikon Eclipse microscope using Image-Pro Plus software (Phase 3 Imaging Systems).

$G8^{pos}$ Cell Ablation in Epithelial Cell Explants. $G8^{pos}$ cell ablation in epithelial explants followed a procedure previously described for ablation of $G8^{pos}$ cells within the epiblast of the chicken embryo (16). For these studies, ex vivo lens epithelial explants were prepared in SFM. On culture day 1, epithelial explants were incubated with G8 antigen (1:20) diluted in Hanks buffered saline for 1 h at 37 °C, followed by incubation in baby rabbit complement (1:40; Cedar Lane) diluted in Hanks buffered saline containing 0.1% BSA for 30 min at room temperature. Baby rabbit complement was prepared according to manufactures protocol (Cedar Lane). Control explants were left untreated or incubated with G8 mAb or complement alone. After treatment, explants were rinsed and incubated with SFM. The presence of lysed G8 cells was determined immediately after treatment by incubating the ex vivo epithelial explants in 0.2% trypan blue in PBS for 15 min at 37 °C and visualized with a dissecting microscope (SMZ800; Nikon) and a Nikon Digital Sight DS-Fi1 camera, and the images were captured using Nikon NIS-Elements imaging software.

Cell Proliferation Assay. Cell proliferation was determined using the Click-iT EdU assay (Invitrogen) according to the manufacturer's instructions. Proliferating cells were labeled for the first hour following injury with EdU (5-ethynyl-2′-deoxyuridine), a nucleoside analog to thymidine. EdU incorporation was detected using the Click-iT EdU Alexa Fluor 488 detection reagent. Nuclei were labeled with TO-PRO-3 (Invitrogen).

Flow Cytometry. Cells were isolated from E15 chicken embryo lens cells with trypsin/EDTA (20 min, 37 °C), labeled with G8 mAb (20 min, 4 °C) followed by fluorescein-conjugated secondary antibody (20 min, 4 °C), fixed with 70% ethanol (4 °C), treated with RNase (0.01 μg/mL, 30 min, 37 °C), and labeled with propidium iodide (PI) (30 min at room temperature). Controls included untreated, an isotype for the G8 Ig (IgM), and secondary antibody alone. DNA content of $G8^{+}$ and $G8^{-}$ cells was determined by flow cytometry analysis using a Coulter Epics XL-MCL (Jefferson Kimmel Cancer Center Core Facility) and analyzed using FlowJo software.

Western Blot Analysis. On day 6, epithelial explants were extracted and lysed in OGT buffer (44.4 mM *n*-Octyl β-D-glucopyranoside, 1% Triton X-100, 100 mM NaCl, 1 mM $MgCl_2$, 5 mM EDTA, 10 mM imidazole) containing a protease inhibitor mixture (Sigma). Protein concentrations were determined with the BCA assay (Pierce). Proteins were separated on Tris-glycine gels (Novex), electrophoretically transferred to membrane (Immobilon-P; Millipore), and immunoblotted. For detection, ECL reagent (Amersham) was used. All gels were run under reducing conditions. Antibodies used for Western blotting included β-actin and α-SMA (Sigma).

ACKNOWLEDGMENTS. We thank Dr. Marilyn Woolkalis for intellectual support and inspiration for this study, Dr. Michelle Leonard for critical reading of the manuscript, Dr. Paul FitzGerald (University of California, Davis) for kindly providing the vimentin polyclonal antibody, and Drs. Peggy Zelenka and Senthil Saravanamuthu (National Eye Institute, National Institutes of Health) for rat newborn lens epithelial explants. This work was supported by National Institutes of Health Grants to A.S.M. (EY014798, EY010577, and EY014258), J.L.W. (EY019571), and M.G.-W. (AR052326).

1. Radisky DC, Kenny PA, Bissell MJ (2007) Fibrosis and cancer: Do myofibroblasts come also from epithelial cells via EMT? *J Cell Biochem* 101:830–839.
2. Eyden B (2008) The myofibroblast: Phenotypic characterization as a prerequisite to understanding its functions in translational medicine. *J Cell Mol Med* 12:22–37.
3. Polyak K, Weinberg RA (2009) Transitions between epithelial and mesenchymal states: Acquisition of malignant and stem cell traits. *Nat Rev Cancer* 9:265–273.
4. Baum B, Settleman J, Quinlan MP (2008) Transitions between epithelial and mesenchymal states in development and disease. *Semin Cell Dev Biol* 19:294–308.
5. Lee JM, Dedhar S, Kalluri R, Thompson EW (2006) The epithelial-mesenchymal transition: New insights in signaling, development, and disease. *J Cell Biol* 172: 973–981.
6. Rønnov-Jessen L, Villadsen R, Edwards JC, Petersen OW (2002) Differential expression of a chloride intracellular channel gene, CLIC4, in transforming growth factor-β1-mediated conversion of fibroblasts to myofibroblasts. *Am J Pathol* 161:471–480.
7. Tomasek JJ, Gabbiani G, Hinz B, Chaponnier C, Brown RA (2002) Myofibroblasts and mechano-regulation of connective tissue remodelling. *Nat Rev Mol Cell Biol* 3: 349–363.
8. Humphreys BD, et al. (2010) Fate tracing reveals the pericyte and not epithelial origin of myofibroblasts in kidney fibrosis. *Am J Pathol* 176:85–97.
9. Brittan M, et al. (2002) Bone marrow derivation of pericryptal myofibroblasts in the mouse and human small intestine and colon. *Gut* 50:752–757.
10. Hashimoto N, Jin H, Liu T, Chensue SW, Phan SH (2004) Bone marrow-derived progenitor cells in pulmonary fibrosis. *J Clin Invest* 113:243–252.
11. Walker JL, Wolff IM, Zhang L, Menko AS (2007) Activation of SRC kinases signals induction of posterior capsule opacification. *Invest Ophthalmol Vis Sci* 48:2214–2223.
12. Gerhart J, et al. (2001) MyoD-positive myoblasts are present in mature fetal organs lacking skeletal muscle. *J Cell Biol* 155:381–392.
13. Strony R, et al. (2005) NeuroM and MyoD are expressed in separate subpopulations of cells in the pregastrulating epiblast. *Gene Expr Patterns* 5:387–395.
14. Gerhart J, et al. (2004) Epiblast cells that express MyoD recruit pluripotent cells to the skeletal muscle lineage. *J Cell Biol* 164:739–746.
15. Bellairs R (1986) The primitive streak. *Anat Embryol (Berl)* 174:1–14.
16. Gerhart J, et al. (2006) MyoD-positive epiblast cells regulate skeletal muscle differentiation in the embryo. *J Cell Biol* 175:283–292.
17. Asakura A, Lyons GE, Tapscott SJ (1995) The regulation of MyoD gene expression: Conserved elements mediate expression in embryonic axial muscle. *Dev Biol* 171: 386–398.
18. Chen JC, Mortimer J, Marley J, Goldhamer DJ (2005) MyoD-cre transgenic mice: A model for conditional mutagenesis and lineage tracing of skeletal muscle. *Genesis* 41: 116–121.
19. Grounds MD, Garrett KL, Beilharz MW (1992) The transcription of MyoD1 and myogenin genes in thymic cells in vivo. *Exp Cell Res* 198:357–361.
20. Gerhart J, et al. (2009) Noggin producing, MyoD-positive cells are crucial for eye development. *Dev Biol* 336:30–41.
21. Davis RL, Weintraub H, Lassar AB (1987) Expression of a single transfected cDNA converts fibroblasts to myoblasts. *Cell* 51:987–1000.
22. Choi J, et al. (1990) MyoD converts primary dermal fibroblasts, chondroblasts, smooth muscle, and retinal pigmented epithelial cells into striated mononucleated myoblasts and multinucleated myotubes. *Proc Natl Acad Sci USA* 87:7988–7992.
23. Gerhart J, et al. (2000) DNA dendrimers localize MyoD mRNA in presomitic tissues of the chick embryo. *J Cell Biol* 149:825–834.
24. Gerhart J, et al. (2004) Visualizing the needle in the haystack: In situ hybridization with fluorescent dendrimers. *Biol Proced Online* 6:149–156.
25. Hinz B, et al. (2007) The myofibroblast: One function, multiple origins. *Am J Pathol* 170:1807–1816.
26. Cattaneo E, McKay R (1990) Proliferation and differentiation of neuronal stem cells regulated by nerve growth factor. *Nature* 347:762–765.
27. Bai Y, Du L, Shen L, Zhang Y, Zhang L (2009) GPR56 is highly expressed in neural stem cells but downregulated during differentiation. *Neuroreport* 20:918–922.
28. Hinz B (2007) Formation and function of the myofibroblast during tissue repair. *J Invest Dermatol* 127:526–537.
29. Mayer DC, Leinwand LA (1997) Sarcomeric gene expression and contractility in myofibroblasts. *J Cell Biol* 139:1477–1484.